

Comparative evaluation of the electrical configurations for the two-dimensional electric potential method of damage monitoring in carbon fiber polymer–matrix composite

Daojun Wang and D D L Chung¹

Composite Materials Research Laboratory, University at Buffalo, State University of New York, Buffalo, NY 14260-4400, USA

E-mail: ddlchung@buffalo.edu

Received 17 October 2005, in final form 13 July 2006

Published 24 August 2006

Online at stacks.iop.org/SMS/15/1332

Abstract

The effectiveness of the two-dimensional electric potential method of damage sensing in a quasi-isotropic carbon fiber polymer–matrix composite depends on the electrical configuration, i.e., the current direction relative to the surface fibers and the electrical contact scheme. Oblique current application in any direction provides effective damage sensing, as shown by using electrical contacts on the opposite in-plane surfaces. In-plane current application through the cross section in any direction also provides effective damage sensing, as shown by using electrical contacts that are either on the edge surfaces or in holes through the composite. In-plane surface current application is effective when the current is perpendicular to the surface fibers (due to the low resistivity in the direction of the fibers) and is ineffective when the current is parallel to the surface fibers (due to the high resistivity in the direction perpendicular to the fibers). The oblique configuration is recommended for practical implementation. In general, the potential method is reliable when (i) the resistance between the electric current line and the nearly parallel electric potential gradient line is sufficiently low, as attained when these lines are sufficiently close, and (ii) the resistance between the current line and the damage location is sufficiently low, as attained when the distance of separation is sufficiently small.

1. Introduction

Damage detection is necessary for composite structural health monitoring (SHM) for space-launch and aerospace flight vehicle structures. The damages appear in different types, levels and locations in composite structural components. The different types, levels and locations of damage have different effects on the fatigue life of a composite structural component under a given fatigue load [1]. It may be relatively easy to predict the fatigue life of a composite structural component

with different damage levels based on a series of laboratory fatigue tests on identical specimens if the damage level is the only controlling factor. However, because of the various effects of the types, levels and locations of damage, it is not reliable to predict the fatigue life of a particular structural component based on laboratory tests in a simplified approach, unless the above factors are considered in a systematic manner. Thus, the monitoring of the location and extent of damage (including all types of damage) of any particular structural component is necessary in order to predict realistically the fatigue life of a composite structural component under a certain operating

¹ Author to whom any correspondence should be addressed.

condition, provided that an identical structural component is being used in the field operation. The need for monitoring is heightened by the aging of the flight vehicles, and especially the 2001 accident of a passenger jet due to a composite joint failure of the vertical tail wing section [2].

Visual inspection and tapping are the most widely used methods of damage assessment of aircraft. However, they are insufficient in sensitivity. Visual inspection cannot detect subsurface flaws, such as subsurface delamination in the fiber composite. In general, flaws do not necessarily initiate at the surface. Moreover, visual inspection cannot detect flaws that are smaller than what the human eyes can see. Tapping can detect subsurface flaws, but only those that are macroscopic.

Ultrasonic inspection [3–5] is more sensitive than visual inspection or tapping, but it is typically limited to flaws that are of size at least a few millimeters. Since a reinforcing fiber in a structural composite is typically around 10 μm in diameter, the breaking of as many of 1000 fibers may escape detection by the ultrasonic technique. In addition, delamination cracks cannot be detected by ultrasonics until the cracks have grown to a sufficiently large size.

Due to the high electrical conductivity of carbon fiber, which is the dominant reinforcement in lightweight polymer–matrix structural composites, the electrical conduction behavior of carbon fiber composites is affected by damage [6–33]. For example, damage in the form of fiber breakage causes the electrical resistivity in the fiber direction of the composite to increase. By DC electrical resistance measurement in one dimension, fiber breakage has been observed to start in carbon fiber epoxy–matrix composites at only half of the fatigue life [27]. A one-dimensional resistance distribution determination, as needed for damage distribution sensing, involves a one-dimensional array of electrical contacts, as illustrated in figure 1(a), where contacts are in the form of strips extending along the entire width of the specimen. In figure 1(a), contacts 1 and 5 are for passing current, while the remaining contacts are to be used two at a time (i.e., 2 + 3, and 3 + 4) for voltage measurement at segments I and II respectively.

In order to obtain information on the damage location, the two-dimensional resistance distribution needs to be determined. This determination ideally involves a two-dimensional array of electrical contacts, as illustrated in figure 1(b) for the case of a 5 × 5 array. However, in practice, the number of electrical contacts is preferably not large. Furthermore, the contacts are preferably near the edge of the specimen, as illustrated in figure 1(c), so that the electrical contacts do not interfere with the usage of the structural component. Therefore, the configuration of figure 1(c) is more suitable for practical implementation than that of figure 1(b).

In order to obtain a considerable amount of information by using a rather small number of electrical contacts, the potential at each contact can be measured (say, relative to ground) for each of a number of directions of current application. This is the conventional procedure, but other procedures of collecting the potential information are possible. An example of the conventional procedure is described below. The current is applied from 1 to 9 (figure 1(c)), while the potential is measured at each of the remaining 14 contacts. After that, the current is applied, say, from 5 to 13, while the potential is measured at each of the remaining 14 contacts. Since

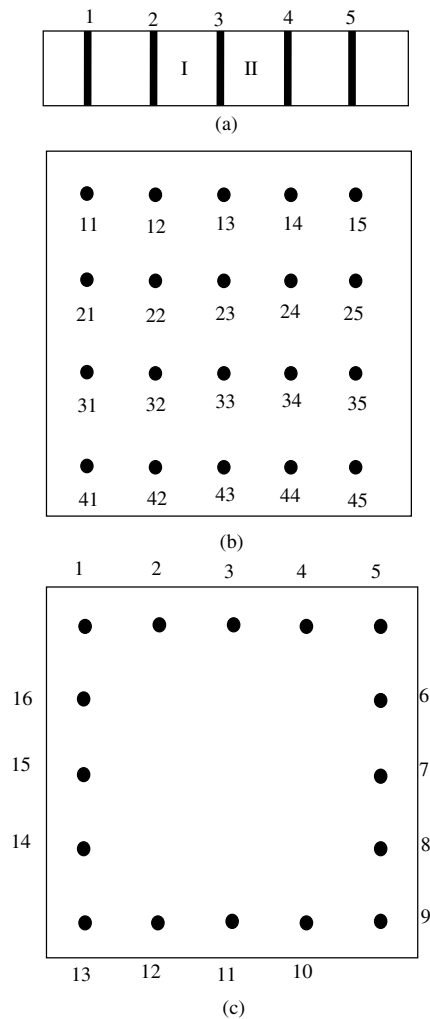


Figure 1. Electrical contact configurations. (a) One-dimensional resistance method. (b) Two-dimensional resistance method. (c) Two-dimensional potential method.

the current line and the potential gradient line (i.e., the line connecting the two points where potential is measured) do not overlap, this two-dimensional method does not correspond to resistance measurement, which involves overlapping of the current line and the potential gradient line. This two-dimensional method is referred to as the potential method.

A damage distribution can be in the form of a region that is damaged, surrounded by a region that is not damaged at all. It can also be in the form of a region of severe damage, surrounded by a region of less damage, such that the severity of the damage in the surrounding region decreases with increasing distance from the region of severe damage. The former scenario applies to localized damage, as in impact damage. The latter scenario applies to delocalized damage, as in flexural damage, in which the flexural stress distribution gives rise to a damage distribution that is spread out.

The sensing of localized damage can be achieved by measuring the resistance of the damaged region. It cannot be achieved by measuring the resistance outside the damaged region, unless the electrical conductivity of the material under study is high enough for the applied current to spread from

the damaged region to the undamaged region. In contrast, the sensing of delocalized damage can be achieved by measuring the resistance in the region of severe damage or the surrounding region of less damage, regardless of the conductivity.

This paper relates to the sensing of localized damage in carbon fiber polymer–matrix composites by using the potential method. A carbon fiber structural composite typically consists of layers (or laminae) of continuous unidirectional carbon fibers. The fibers can be in different directions for the different laminae. For example, a quasi-isotropic lay-up configuration with 24 laminae can be $[0/45/90/-45]_{3s}$. Although the lay-up is quasi-isotropic, the surface fibers are unidirectional and are in the 0° direction. In general, the fibers on the surface where the electrical contacts most conveniently reside are all in a particular direction, whatever is the lay-up configuration.

The data obtained by the two-dimensional potential method depend on the extent of current spreading, which necessarily occurs between two point contacts on a two-dimensional conductive surface. As the conductivity is much higher in the plane than in the through-thickness direction of the composite, current spreading mainly occurs two-dimensionally. It has been reported that the current spreading occurs to a distance of 500 mm in the 0° direction [31]. The extent of current spreading increases with decreasing electrical resistivity in the direction of the spreading, i.e., the direction (on the plane) perpendicular to the straight line connecting the two current contacts. Due to the unidirectional nature of the surface fibers and the consequent in-plane anisotropy of the surface resistivity of the composite, the extent of current spreading is expected to depend strongly on the direction in the case of surface current application. For example, surface current in the 0° direction (i.e., the direction of the surface fibers) is expected to spread less than current in the 90° direction. In the case of current that is applied to all the laminae, as attained by using current that cuts through all the laminae (such as current in the oblique direction, i.e., current at an angle greater than 0° and less than 90° from the plane of the laminate) or by using current that runs along all the laminae (due to current contacts that touch all the laminae), the current spreading will be more isotropic in the plane of the laminate. Isotropic current spreading in the plane of the laminate is ideal for the two-dimensional potential method.

The anisotropic current spreading (which depends on the current direction in relation to the fiber orientation) complicates the design of the electrical configuration (particularly the electrical contact scheme) for conducting the two-dimensional potential method. The current direction can be in the plane of the composite or be in an oblique direction (a direction between the in-plane direction and the through-thickness direction). For the case of the current in the plane of the composite, the current may be on the surface or be throughout the cross section. There are also various choices of the electrical contact scheme. Although the two-dimensional potential method has been previously used for damage location determination of carbon fiber epoxy–matrix composites [29, 34–36], the effect of the electrical configuration has received little attention [36].

The way that current is applied is governed by the electrical contact configuration. The configurations include (i) that in which the current contacts are on the same surface

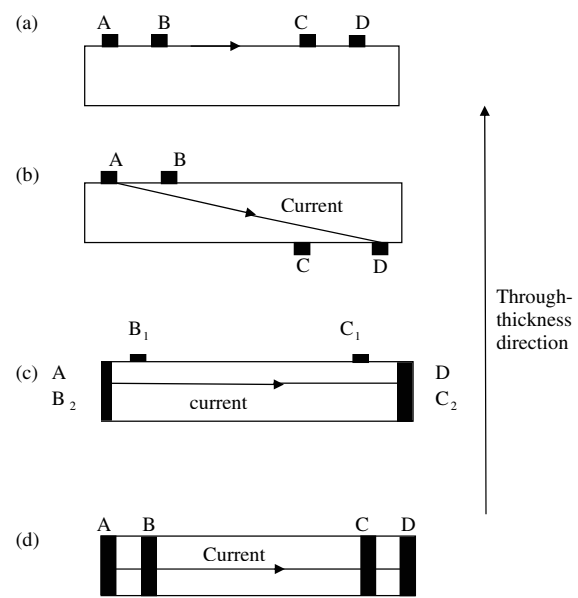


Figure 2. Electrical contact configurations.

in the plane of the laminate, so that the current is in the surface region only (figure 2(a)), (ii) that in which the current contacts are on opposite surfaces in the plane of the laminate, such that they are not directly opposite one another, thereby providing an oblique current (figure 2(b)), (iii) that in which the current contacts are on the edge surfaces (surfaces that are perpendicular to the plane of the laminate), so that the current is in the plane of the laminate and goes through the entire cross section of the specimen (figure 2(c)), and (iv) that in which the current contacts are in holes that are through the thickness of the laminate, so that the current is in the plane of the laminate and goes through the entire cross section of the specimen (figure 2(d)).

Reference [36] uses an electrical configuration similar to that of figure 2(a), but differs from that of figure 2(a) in that the contacts A and D are on the opposite surface from contacts B and C. This means that reference [36], as in figure 2(a), involves the application of a surface current. Reference [36] does not address the electrical configurations of figures 2(b), (c) or (d).

This paper provides a comparative study of the electrical configurations, with the aim of arriving at a configuration that results in greatest effectiveness for practical implementation of the two-dimensional potential method. A quasi-isotropic lay-up configuration was chosen for this study, due to the wide usage of this configuration in structures.

2. Experimental methods

Commercially manufactured composites in the form of continuous carbon fiber (Hexcel IM7, a high-performance intermediate-modulus, PAN-based fiber, with diameter $5\ \mu\text{m}$, 12 000 fibers per tow and tensile modulus 290 GPa) epoxy–matrix (CYCOM 977-3 toughened epoxy resin with a curing temperature of 177°C) laminates of thickness 3.2 mm were cut into specimens of length 120 mm (in the 0° , 45° or 90°

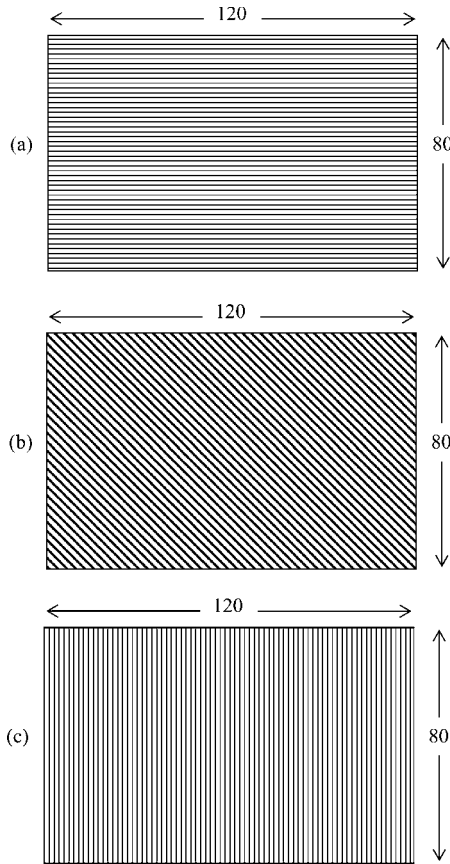


Figure 3. Orientation of the surface fibers in specimens. (a) 0° orientation. (b) 45° orientation. (c) 90° orientation. All dimensions are in mm.

direction) and width 80 mm, as illustrated in figure 3. In other words, one orientation (referred to as the 0° orientation) has the surface fibers along the 120 mm length of the specimen (figure 3(a)); another orientation (referred to as the 90° orientation) has the surface fibers along the 80 mm width of the specimen (figure 3(c)); yet another orientation (referred to as the 45° orientation) has the surface fibers at an angle of 45° from the 120 mm length of the specimen (figure 3(b)). The specimens were then sanded by using 600 grit silicon carbide sand paper for the purpose of removing the surface layer (about 20 μm thick) of epoxy matrix prior to the application of electrical contacts. The contacts were in the form of silver paint in conjunction with copper wire.

The sanding step is not essential, but it helps the electrical measurement by increasing the accuracy and decreasing the noise. Although the entire surface was sanded in this work, only the portions beneath the electrical contacts needed to be sanded. The laminate had 24 laminae in the quasi-isotropic [0/45/90/−45]_{3s} lay-up configuration.

Two sets (labeled I and II) of voltage contacts were used. Set I consisted of ten contacts (labeled 1, 2, . . . , 10, figure 4). For the configuration of figure 2(a), all ten contacts were on the surface which was to receive impact for the purpose of damage infliction. For the configuration of figure 2(b), contacts 1–5 were on the surface which was to receive the impact and contacts 6–10 were on the opposite surface. For the

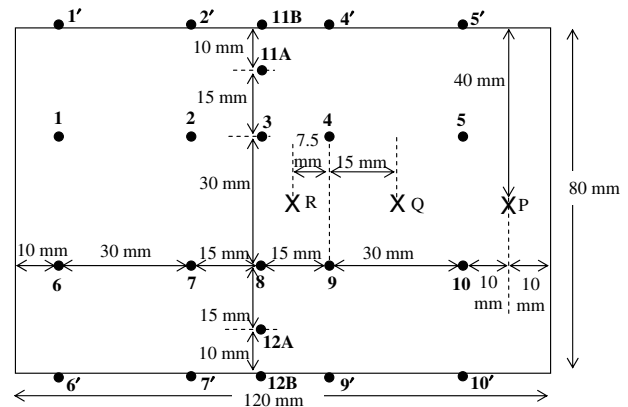


Figure 4. Specimen configuration for investigating the two-dimensional potential method. 1, . . . , 10 are the set I voltage contacts; 1', . . . , 10' are the set II voltage contacts; 11A and 12A are the set A current contacts; 11B and 12B are set B current contacts. The point of impact was successively at P, Q and R.

configuration of figure 2(d), all ten contacts were through the entire thickness, as enabled by drilled holes (1 mm diameter) with a protruding stranded tin-coated copper wire (42 strands in the 18 AWG wire, with each strand of diameter 0.16 mm and AWG 34) in each hole and silver epoxy (a commercial silver particle filled epoxy resin) both between the wire and the wall of each hole and among the strands of each wire. (The use of silver paint together with a non-conductive epoxy overlayer in place of silver epoxy for the through-hole contacts does not provide electrical contacts that are sufficiently stable mechanically, so the resulting data are noisy and are not included in this paper.) For the configurations of figures 2(a) and (b), each of the contacts in set I was in the form of a dot made from silver paint and of diameter 3 mm. Set II voltage contacts (for the configuration of figure 2(c)) consisted of eight contacts (labeled 1', 2', 4', 5', 6', 7', 9' and 10', figure 4), which were in the form of strips applied on the edge surface in the through-thickness direction, such that each strip was of width 3 mm and extended for the whole thickness of the laminate.

Two sets of current contacts were used separately. Set A allowed surface (in the plane of the laminate) or oblique current application and consisted of contacts 11A and 12A, which were on the surface of the laminate (figure 4). For surface current application (configuration of figure 2(a)), contacts 11A and 12A were on a surface which was to receive impact. For oblique current application (configuration of figure 2(b)), contact 11A was on the surface which was to receive impact, while contact 12A was on the opposite surface. Set B was for the configuration of figure 2(c) and consisted of contacts 11B and 12B (figure 4), which were strips on the edge surface in the through-thickness direction, such that each strip was of width 3 mm and extended for the entire thickness of the laminate.

In order to enhance the mechanical integrity, each current or voltage contact (except those involving silver epoxy) was covered with an epoxy (non-conductive) coating after the silver paint had dried. For each set of current contacts, the voltage at each of the voltage contacts of set I (1–10) was measured relative to ground. After that, the difference in voltage between selected potential contacts was calculated.

The voltage difference between two potential contacts, divided by the distance between these contacts, is referred to as the potential gradient, which describes the average potential gradient over the distance between the two potential contacts. The potential gradient may not be uniform over this distance, since the damage distribution may not be uniform. The determination of the potential distribution [36] is not the method used in this work for damage sensing. Rather, this work uses the average potential gradient (referred to as the potential gradient) between selected electrical contact points for damage sensing. The advantage of the method used in this work is that only a small number of electrical contacts are needed. In contrast, a large number of electrical contacts (e.g., 121 [36]) in a two-dimensional array are required in the determination of the potential distribution. Due to the impracticality of having an array of electrical contacts covering most of the surface of a composite panel, the method of damage sensing involving the determination of the potential distribution is not attractive.

The voltage at each of the voltage contacts of set II (1', 2', etc) was also measured by using the set B current contacts. Thus, three electrical measurement schemes were used, namely (i) set A current contacts along with set I voltage contacts, (ii) set B current contacts along with set I voltage contacts, and (iii) set B current contacts along with set II voltage contacts.

Before, during and after impact using a steel hemisphere (19 mm or 0.75 in diameter) dropped from a controlled height, potential measurement was made with a fixed DC current (50, 75 or 100 mA, as noted). The hemisphere was manually arrested during the rebound after an impact. The impact energy was calculated from the weight of the ball assembly (either 0.740 or 2.640 kg) and the initial height of the ball (up to 760 mm). The impact was directed at the same point of the specimen at progressively increasing energy. The point of impact was successively at P, Q and R (figure 4). Hence, the location (center) of the damage was well-defined. The cumulative damage was analyzed. Although cumulative damage is more than damage resulting from a single impact at the maximum impact energy used in inflicting cumulative damage, it is meaningful in providing the damage evolution for the same specimen as the impact energy progressively increased.

All the data presented in this paper were obtained on (i) two specimens in the 0° orientation (one specimen with set A current contacts, set I voltage contacts and the configuration of figure 2(a); the other specimen with set A current contacts, set I voltage contacts and the configuration of figure 2(b)), (ii) five specimens in the 90° orientation (one specimen with set A current contacts, set I voltage contacts, and the configuration of figure 2(a); a second specimen with set A current contacts, set I voltage contacts and the configuration of figure 2(b); a third specimen with set B current contacts, set I voltage contacts, and the configuration of figure 2(c); a fourth specimen with set B current contacts, set II voltage contacts and the configuration of figure 2(c); a fifth specimen with set A current contacts, set I voltage contacts and the configuration of figure 2(d)) and (iii) one specimen in the 45° configuration, with set A current contacts, set I voltage contacts and the configuration of figure 2(a). Testing had been performed on multiple specimens of each type in order to confirm the general reproducibility of the results.

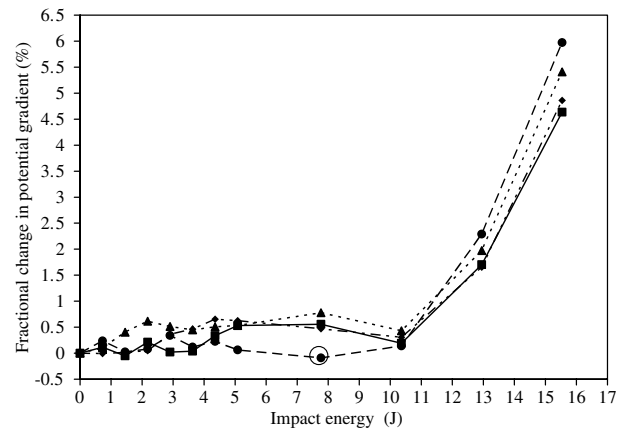


Figure 5. Fractional change in potential gradient (relative to the value prior to any impact) versus impact energy, which was progressively increased for the 0° orientation. Set A current contacts were used along with set I voltage contacts. The configuration is that of figure 2(a). The current is 75 mA. Impact was directed at point P. The different sets of data are for different potential gradient lines. ■: line 1–7; ◆: line 2–8; ▲: line 3–9; ●: line 4–10. The circled data point may be a little off due to a data acquisition problem.

3. Results and discussion

3.1. Configuration of figure 2(a)

In this section, set A current contacts were used along with set I voltage contacts. The configuration is that of figure 2(a). Figure 5 shows the results for the 0° orientation with the point of impact at P. Data are shown for the fractional change in potential gradient at lines 1–7, 2–8, 3–9 and 4–10, which are all at an angle to the current line 11A–12A. Among these potential gradient lines, line 4–10 is closest to the point of impact, and it gives the highest fractional change in potential gradient for the same high impact energy of 13 J or above. At 15 J, the fractional change in potential gradient decreases in the order 4–10, 3–9, 2–8 and 1–7, i.e., it decreases with increasing distance from the point of impact. However, at 10 J and below, the fractional change in potential gradient is highest for 3–9 and 2–8, due to their proximity to the current line. Thus, the sensitivity for damage monitoring is best for potential gradient lines that are closest to the damage location when the damage is major, but is best for potential gradient lines that are closest to the current line when the damage is minor.

Figure 6 shows that, for the 0° orientation, impact at point P increased the potential gradient, such that the fractional increase was higher for greater proximity of the potential gradient line with the point of damage infliction (figure 6(a)). Subsequent impact at point Q increased the potential gradient further, due to the additional damage, and the fractional increase in potential gradient was again higher for greater proximity of the potential gradient line with the point of maximum damage (figure 6(b)). However, still subsequent impact at point R gave relatively little additional increase in the potential gradient and the increase was not monotonic with increasing impact energy (figure 6(c)). This means that the ability to distinguish between different extents of damage is small when the damage is very extensive, as is the case after impact at both points P and Q.

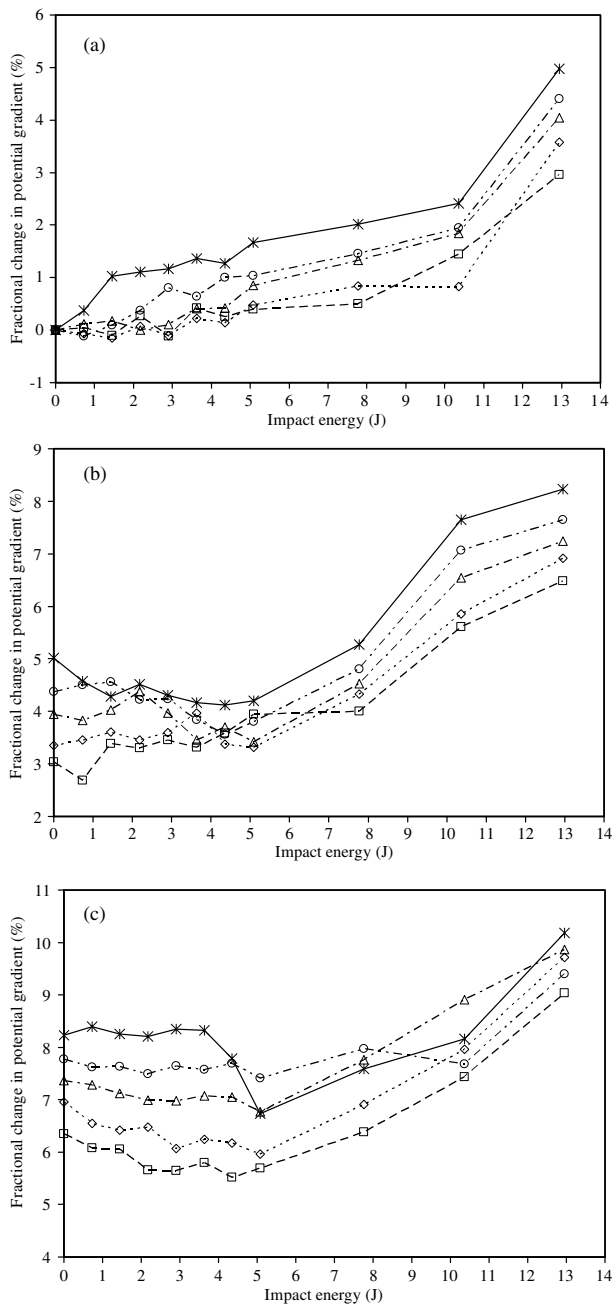


Figure 6. Fractional change in potential gradient (relative to the value prior to any impact) versus impact energy for the 0° orientation. Set A current contacts were used along with set I voltage contacts. The configuration is that of figure 2(a). The current is 50 mA. Impact was directed successively at points P (a), Q (b) and R (c), such that the impact energy was progressively increased for each point of impact. The potential gradient lines are 5–10 (*), 4–9 (O), 3–8 (Δ), 2–7 (\diamond) and 1–6 (\square).

Corresponding results for the 90° orientation (not shown) show large and non-systematic variation of the potential gradient with impact energy for impact at P, Q or R. Thus, the damage sensing failed for the 90° orientation. Large and non-systematic variation had been previously observed when the current and potential gradient lines are at a distance of 2.1 mm or more in the through-thickness direction [37].

Figure 7 shows comparison of the corresponding results for the 0° and 90° orientations, with the point of impact at P. Line 3–8 (figure 7(a)) shows essentially no sensitivity to damage for the 90° orientation, as indicated by the fractional change in potential gradient remaining close to zero up to the highest impact energy of 13 J. On the other hand, for the 0° orientation, line 3–8 shows non-zero fractional change in potential gradient, such that this fractional change increases with increasing impact energy, starting with a low impact energy of 1 J. This means that the 90° orientation using line 3–8 is unable to sense the damage at P, due to the substantial resistance between line 3–8 and the point of impact.

Lines 2–7 (figure 7(b)), 4–9 (figure 7(c)), 1–6 (figure 7(d)) and 5–10 (figure 7(e)) show large but non-systematic variation of the potential gradient with impact energy for the 90° orientation, again with the point of impact at P. In contrast, for the 0° orientation with the same point of impact, the variation is small and systematic (figures 5 and 7). The difference in scale of the vertical axis between figures 5 and 7 is to be noted. This means that the 90° orientation using lines 2–7, 4–9, 1–6 and 5–10 is unable to sense the damage at A. Furthermore, the large and non-systematic variation of the potential gradient with impact energy means that the potential method for the 90° orientation is prone to giving results that are not meaningful.

For the 45° orientation, the potential gradient variation with impact energy is small and somewhat systematic, unlike the large and non-systematic variation for the 90° orientation. Figure 8 shows the variation for the 45° orientation, as obtained by using set A current contacts and set I voltage contacts during impact at P at progressively increasing energy. Comparison between figures 8 and 6(a), both for impact at P, shows that the variation is smaller and less systematic for the 45° orientation than the 0° orientation.

In general, the potential method involving surface current application is reliable only when the current and potential gradient lines are sufficiently close, so that the resistance between them (in the direction perpendicular to these lines) is sufficiently low. When this direction is the 0° direction (i.e., the fiber direction of the surface lamina), the current and potential gradient lines can be as much as 45 mm apart (distance between lines 1 and 6 and 11A and 12A in figure 4). The maximum possible distance is probably much more than 45 mm, due to prior work that indicated 0° current spreading by a distance of 500 mm [31]. When this direction is the 90° direction (i.e., the transverse direction of the surface lamina), the current and potential gradient lines must be less than 15 mm apart. The maximum possible distance is less than 15 mm and has not been determined. When this direction is the through-thickness direction, the current and potential gradient lines need to be less than 2.1 mm apart [37].

The potential method is sensitive to damage only when the current line is sufficiently close to the location of the damage, so that the resistance between them is sufficiently small. When the current line is perpendicular to the 0° direction, the distance between the current line and the point of impact can be as much as 55 mm (distance between line 11A and 12A and point P in figure 4). The maximum possible distance is probably much more than 55 mm, due to the 0° current spreading by 500 mm [31]. When the current line is in the 0° direction, the distance must be less than 7.5 mm (distance between line 11A

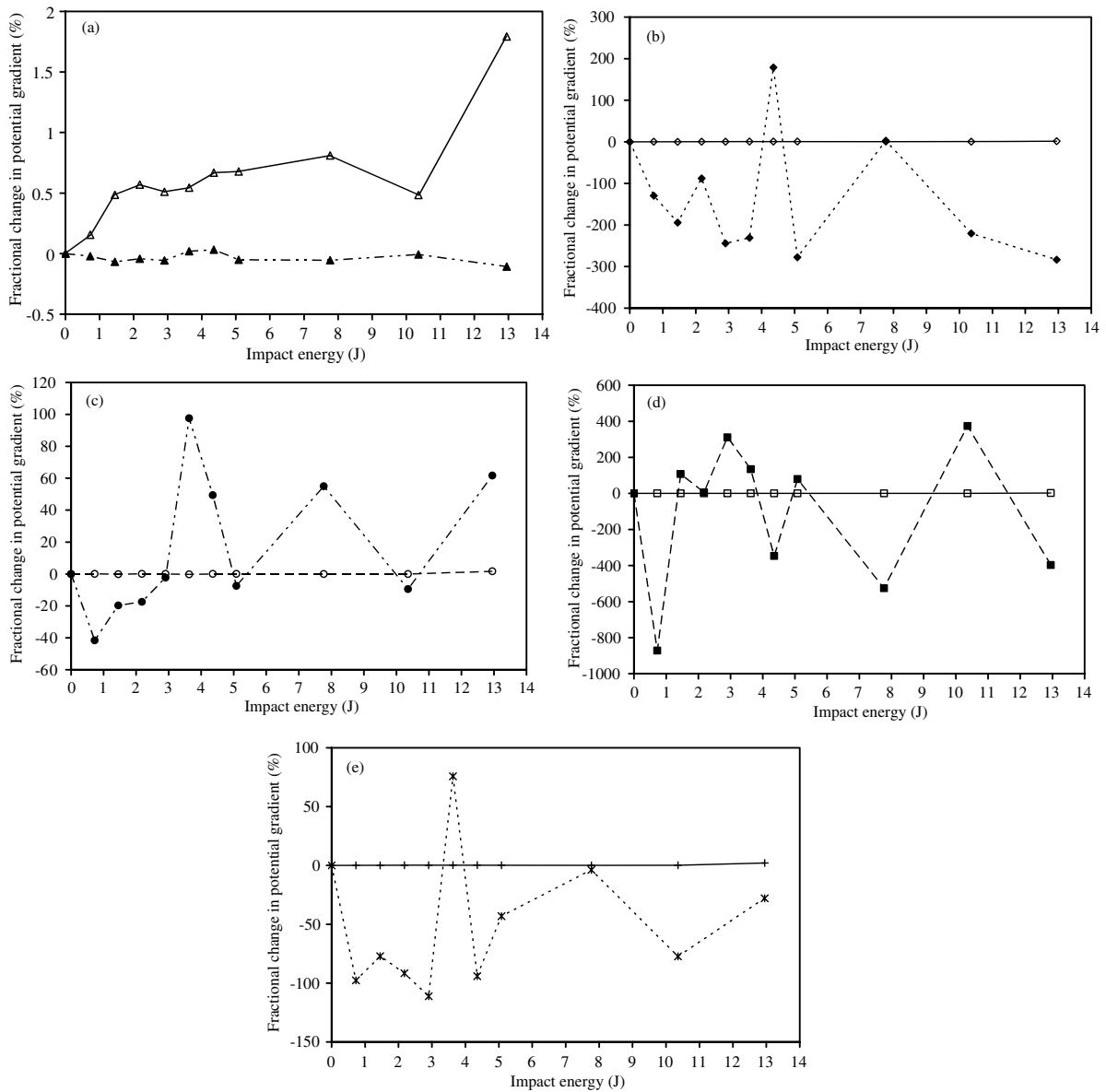


Figure 7. Fractional change in potential gradient (relative to the value prior to any impact) versus impact energy, which was progressively increased. Set A current contacts were used along with set I voltage contacts. The configuration is that of figure 2(a). The current is 50 mA. Impact was directed at point P. (a) The potential gradient line is 3–8; Δ : 0° orientation; \blacktriangle : 90° orientation. (b) The potential gradient line is 2–7; \diamond : 0° orientation; \blacklozenge : 90° orientation. (c) The potential gradient line is 4–9; \circ : 0° c orientation; \bullet : 90° c orientation. (d) The potential gradient line is 1–6; \square : 0° c orientation; \blacksquare : 90° orientation. (e) The potential gradient line is 5–10; $+$: 0° orientation; $*$: 90° orientation.

and 12A and point R). The maximum possible distance is less than 7.5 mm and has not been determined.

The distance limitations are severe in the 90° direction. As a result, practical use of the two-dimensional potential method with surface current application, involving the electrical contact scheme illustrated in figure 1(c), should avoid data corresponding to the 90° orientation. For example, data obtained by using current line 15–7 and potential gradient line 14–8 should be avoided (figure 1(c)), if the 0° direction (i.e., fiber direction of the surface lamina) is in the 15–7 direction. The avoiding of data corresponding to the 90° orientation makes the two-dimensional potential method not fully two-dimensional, thus limiting the effectiveness of this method. Furthermore, the avoiding of these data means that the conventional procedure of data collection in the two-

dimensional potential method, as described in the introduction, needs modification in the case of surface current application. This problem stems from the unidirectionality of the fibers in the surface lamina.

In [36], the current line goes through the location of the damage, although the current is on the opposite surface from the surface receiving the impact. As a result, in-plane current spreading from the current line to the location of damage is not necessary and the potential method of [36] allows damage sensing for the 90° configuration. In the 90° configuration of [36], the relatively small extent of current spreading in the direction perpendicular to the surface fibers makes the determination of the damage location in this direction relatively accurate.

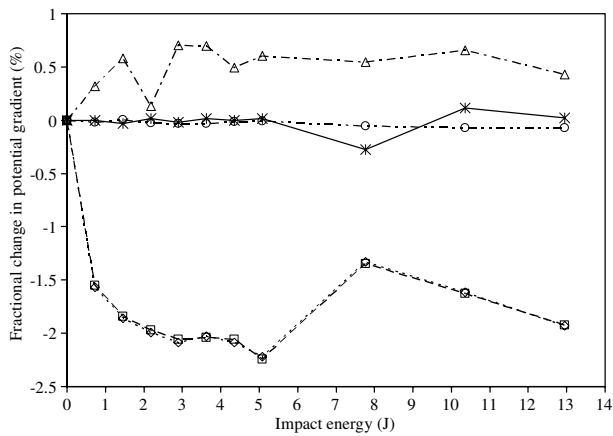


Figure 8. Fractional change in potential gradient versus impact energy for the 45° orientation. Set A current contacts were used along with set I voltage contacts. The configuration is that of figure 2(a). The current is 50 mA. Impact was directed at point P, such that the impact energy was progressively increased. The potential gradient lines are 5–10 (*), 4–9 (O), 3–8 (Δ), 2–7 (\diamond) and 1–6 (\square).

The configuration of [36] is similar to that of figure 2(a) in that the electrical contacts for potential measurement are on the surface receiving the impact (the top surface). However, the current is applied on the bottom surface in [36], whereas the current is applied on the top surface in figure 2(a).

Although the current is applied between two points on the bottom surface in [36], the current spreads in both the in-plane and through-thickness directions of the quasi-isotropic or cross-ply composite laminate, thus resulting in current at the top surface that is more spread out in the plane of the laminate than the current at the bottom surface. An additional factor is that the current line goes through the location of the damage [36]. As a result, for attaining damage sensing, the need for current spreading is relatively small in [36] compared to the configuration of figure 2(a).

Reference [36] reports that the 0° configuration does not allow damage sensing. The ineffectiveness of the 0° configuration in [36] is attributed to (i) the current spreading along the surface fibers making the potential relatively uniform in this direction and this potential uniformity overshadowing the effect of damage on the potential, and (ii) the high surface resistance in the direction perpendicular to the surface fibers (due to the large role of the polymer matrix) making the potential gradient change in the direction perpendicular to the surface fibers not very sensitive to the damage.

In practical application, the current line typically does not go through the location of damage, since the damage can be anywhere in the plane of the laminate. Therefore, the case addressed in [36], with the current line going through the location of the damage, is a restricted one. In contrast, this work addresses the general case in which the current line does not go through the location of the damage.

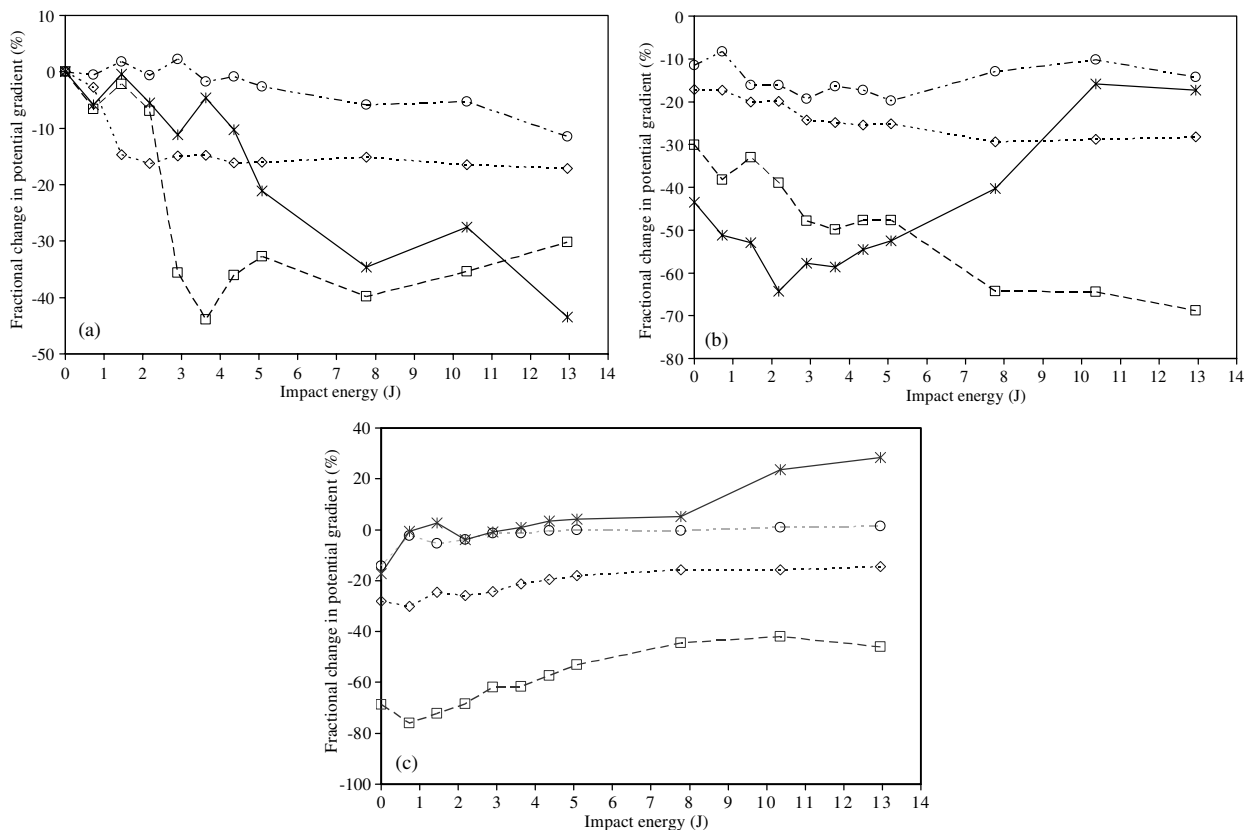


Figure 9. Fractional change in potential gradient (relative to the value prior to any impact) versus impact energy for the 90° orientation. Set B current contacts were used along with set II voltage contacts. The configuration is that of figure 2(c). The current is 50 mA. Impact was directed successively at points P (a), Q (b) and R (c), such that the impact energy was progressively increased for each point of impact. The potential gradient lines are 5–10 (*), 4–9 (O), 2–7 (\diamond) and 1–6 (\square).

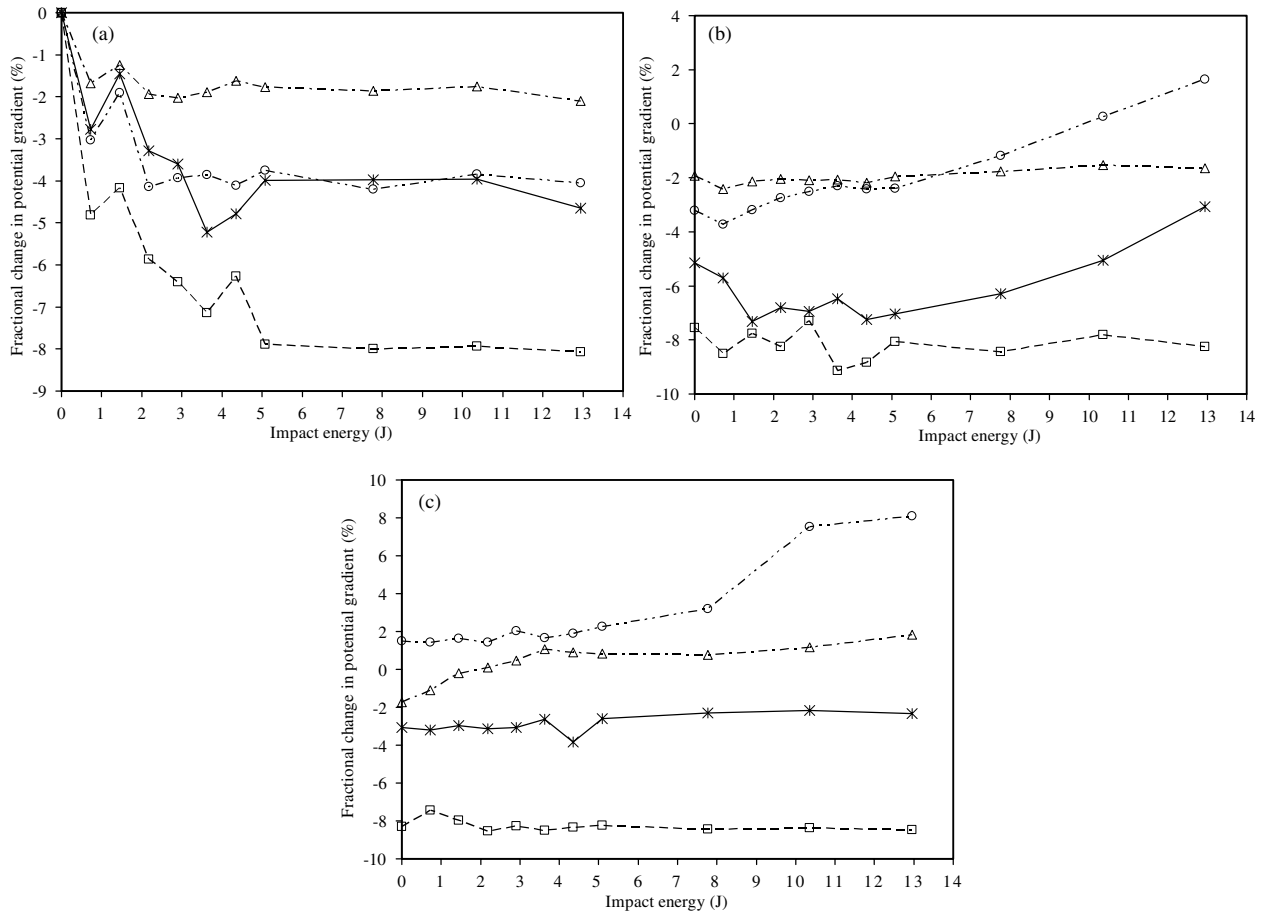


Figure 10. Fractional change in potential gradient (relative to the value prior to any impact) versus impact energy for the 90° orientation. Set A current contacts were used along with set I voltage contacts. The configuration is that of figure 2(d). The current is 100 mA. Impact was directed successively at points P (a), Q (b) and R (c), such that the impact energy was progressively increased for each point of impact. The potential gradient lines are 5–10 (*), 4–9 (O), 2–7 (Δ) and 1–6 (□).

In general, current spreading helps the detection of damage that is away from the line of current application. When the damage is localized and the current line is away from the damage region, current spreading is essential. However, current spreading reduces the accuracy of the damage location determination, since it causes the potential to be more uniform. Thus, in practice, a compromise is recommended.

If the goal is the detection of damage that can be anywhere in the laminate, current spreading must be sufficient. If the goal is the detection of damage at a specific location, current that goes through the location should be applied and current spreading is then not important.

3.2. Configuration of figure 2(c), with surface voltage measurement

In this section, set B current contacts were used along with set I voltage contacts. The configuration is that of figure 2(c), with voltage contacts B₁ and C₁. For impact at each of points P, Q and R in the 90° orientation, the variation of the potential gradient with impact energy is non-systematic, as in figures 7(b)–(e). This means that the use of current applied to all the laminae (figure 2(c)) in place of surface current

application did not solve the problem of ineffective damage sensing for the 90° orientation.

3.3. Configuration of figure 2(c), with voltage measured at all the laminae

In this section, set B current contacts were used along with set II voltage contacts. The configuration is that of figure 2(c), with voltage contacts B₂ and C₂. The variation of the potential gradient with impact energy was systematic for the 90° orientation, as shown in figure 9. In the regime of minor damage, as for impact at point P only (figure 9(a)), the potential gradient decreased with increasing impact energy. This is probably because of the resistivity decrease resulting from increase in the degree of fiber waviness—a consequence of the disturbance associated with the damage. In the regime of major damage, as for impact at point Q (figure 9(b)) and point R (figure 9(c)), the potential gradient increased with increasing impact energy, as expected. This damage may be in the form of matrix cracking between the fibers. In figure 9(b), the potential gradient at line 5–10 (close to points P and Q) decreased with increasing impact energy at energy below 2 J, but increased with increasing impact energy above 2 J. This is because of

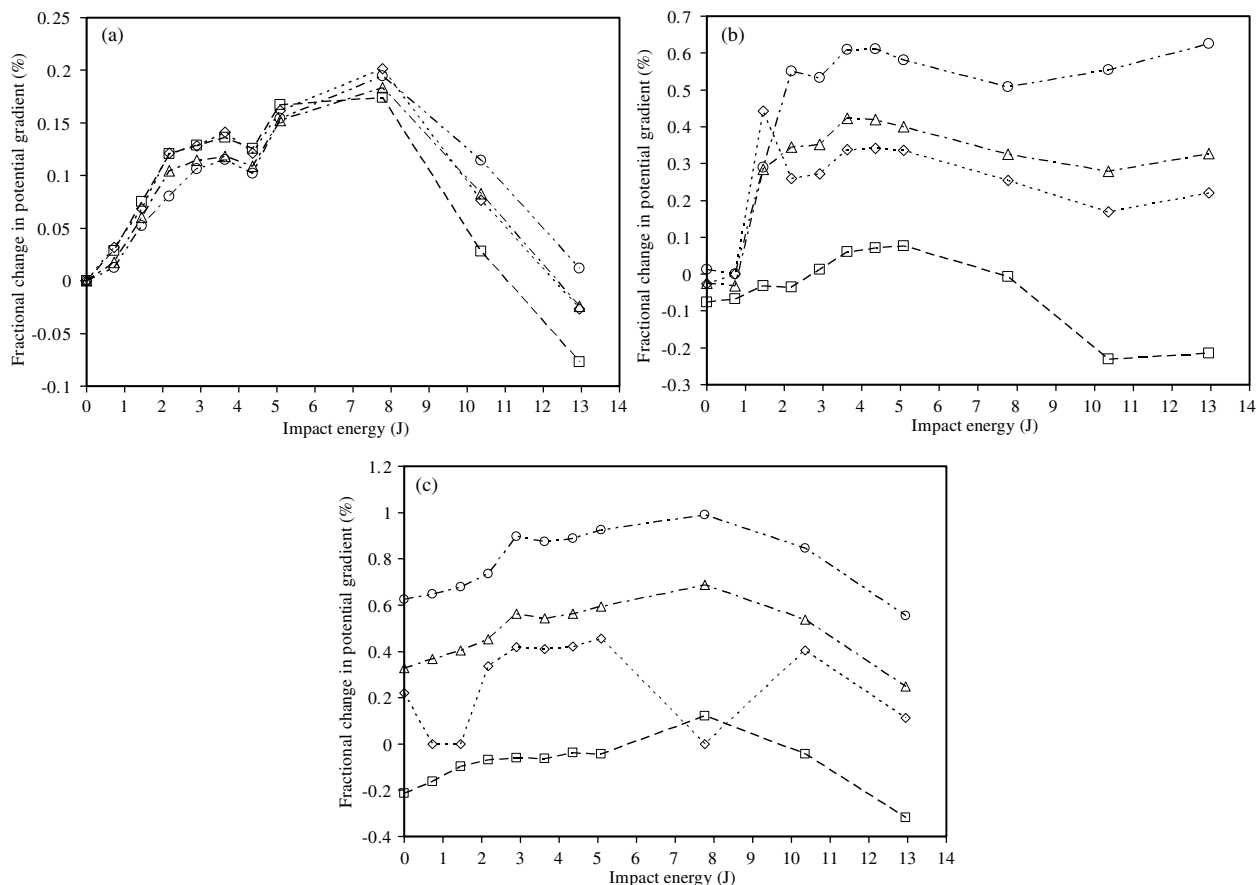


Figure 11. Fractional change in potential gradient (relative to the value prior to any impact) versus impact energy for the 0° orientation. Set A current contacts were used along with set I voltage contacts. The configuration is that of figure 2(b). The current is 100 mA. Impact was directed successively at points P (a), Q (b) and R (c), such that the impact energy was progressively increased for each point of impact. The potential gradient lines are 4–9 (○), 3–8 (△), 2–7 (◇) and 1–6 (□).

the change from behavior that characterized minor damage to behavior that characterized major damage. Line 4–9 is farther away from P and Q (together constituting the center of overall damage) than line 5–10, so line 4–9 experienced less damage than line 5–10, thus not showing the change in behavior until 5 J in figure 9(b). Lines 2–7 and 1–6 are even farther away from P and Q than line 4–9, so they did not show the change in behavior until impact was inflicted at R (figure 9(c)).

3.4. Configuration of figure 2(d)

In this section, set A current contacts were used along with set I voltage contacts. The configuration is that of figure 2(d). The specimens was in the 90° orientation. (The 0° orientation was not addressed, because the 90° orientation is the one that may pose a problem.) Minor damage causes the potential gradient to decrease, as shown in figure 10(a) for impact at point P at progressively increasing energy. Major damage causes the potential gradient to increase, as shown in figures 10(b) and (c) for impact at points Q and R respectively. This behavior is similar to that in figure 9, which is for the configuration of figure 2(c), with set B current contacts and set II voltage contacts.

3.5. Configuration of figure 2(b)

In this section, set A current contacts were used along with set I voltage contacts. The configuration is that of figure 2(b).

For the specimen in the 0° orientation, minor damage caused the potential gradient to increase, whereas major damage caused the potential gradient to decrease, as shown in figure 11(a). That potential gradient increase was observed at low impact energies for each of the successive impact points of P (figure 11(a)), Q (figure 11(b)) and R (figure 11(c)) suggests that fresh minor damage, as obtained by impacting at a previously undamaged point, gives rise to an increase in the potential gradient. In contrast, for the case of the configuration of figure 2(a), with set A current contacts and set I voltage contacts (also the 0° orientation), the potential gradient mainly increases with impact energy, whether the impact is at P, Q or R (figure 6). The difference between the behavior in figures 11 and 6 is attributed to (i) major damage tending to decrease the oblique resistivity, due to the increased contact between fibers of adjacent laminae, and (ii) impact damage tending to increase the resistivity of the surface lamina in the plane of the lamina. The increase of the oblique potential gradient at low impact energies is attributed to the increase in the oblique resistance, as caused by the damage suffered by the lamina or laminae near the surface receiving the impact.

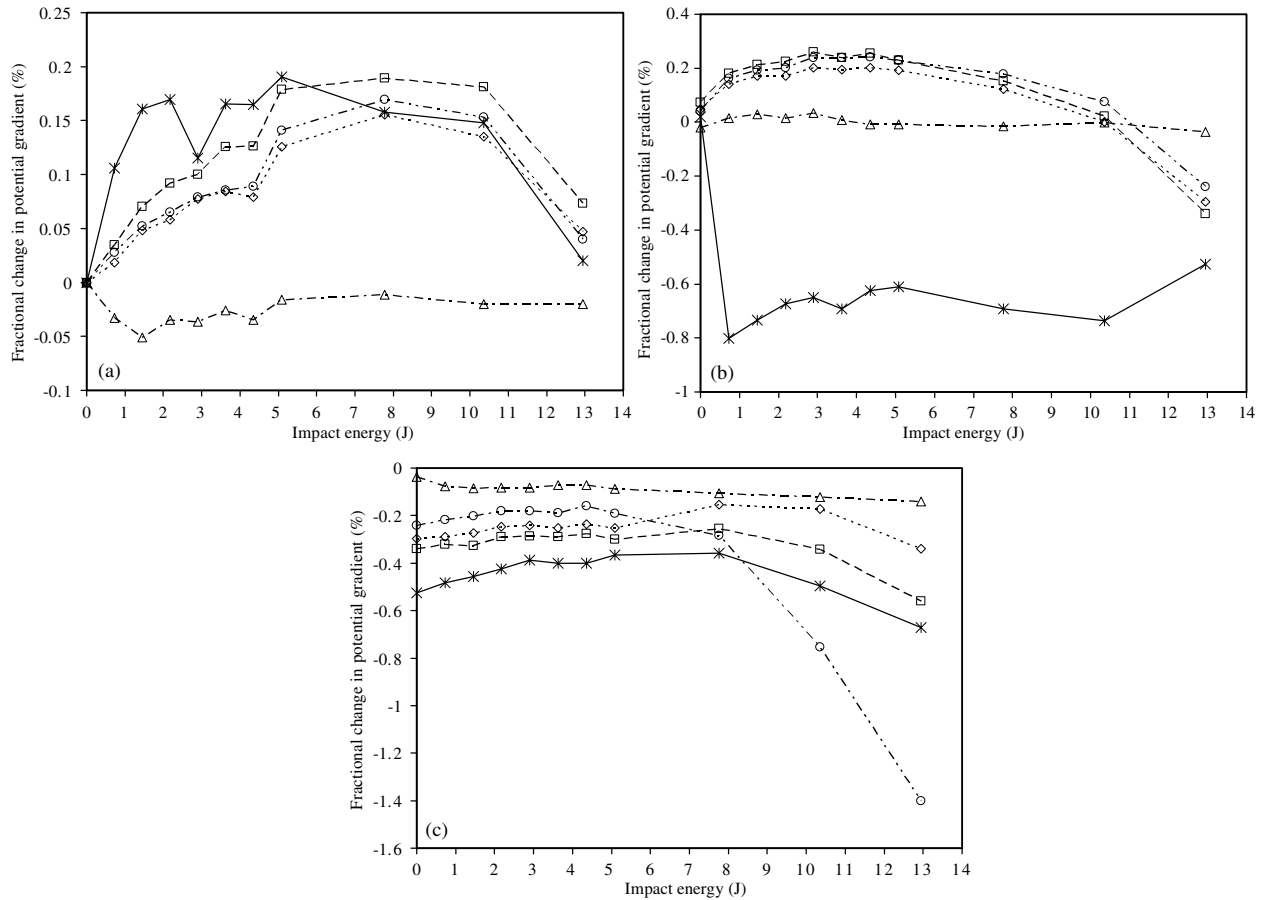


Figure 12. Fractional change in potential gradient (relative to the value prior to any impact) versus impact energy for the 90° orientation. Set A oblique current contacts were used along with set I voltage contacts. The configuration is that of figure 2(b). The current is 100 mA. Impact was directed at P, such that the impact energy was progressively increased. The potential gradient lines are 5–10 (*), 4–9 (O), 3–8 (Δ), 2–7 (\diamond) and 1–6 (\square).

For the configuration of figure 2(b) in the 90° orientation (figure 12), the potential gradient at lines 1–6, 2–7, 4–9, and 5–10 increased with impact (at point P, figure 12(a)) at energy from 5 to 10 J and decreased at 13 J. This behavior is similar to that for the 0° orientation (figure 11(a)). However, for the 90° orientation, the potential gradient at line 3–8 (essentially in line with the current line) did not show any change. Subsequent impact at point Q (figure 12(b)) and then point R (figure 12(c)) gave similar decrease of the potential gradient at lines 1–6, 2–7, 4–9 and 5–10, and similar absence of change for the potential gradient at line 3–8. The fractional change in potential gradient was small compared to that in figure 9(a) (configuration of figure 2(c), with voltage measured at all the laminae and the 90° orientation). The configuration of figure 2(b) is more suitable for practical implementation than that of figure 2(c), since the edge surface involved with the contact configuration for figure 2(c) is usually not accessible in a composite structure.

4. Conclusion

The effectiveness of the potential method for any direction of current application is needed for the method to be truly two-dimensional. In-plane surface current application in the 90°

direction (i.e., the 0° orientation, with current spreading in the 0° direction, which is the direction of low resistivity), in conjunction with surface voltage measurement, is effective for damage sensing. In-plane surface current application in the 45° direction in conjunction with surface voltage measurement gives results that have little sensitivity to damage. In-plane surface current application in the 0° direction (i.e., the 90° orientation, with current spreading in the 90° direction, which is the direction of high resistivity) in conjunction with surface voltage measurement gives wild data, i.e., large and non-systematic variation of the potential gradient with the impact energy. Application of 0° current to all the laminae (by using current contacts on the edge surface), in conjunction with in-plane surface voltage measurement, is also ineffective. On the other hand, application of 0° current to all the laminae by using current contacts on the edge surface, in conjunction with voltage measurement at all the laminae by using voltage contacts on the edge surface, is effective, as shown by the potential gradient decreasing with increasing impact energy in the regime of minor damage and increasing with increasing impact energy in the regime of major damage. Application of 0° current to all the laminae by using through-hole current and voltage contacts is also effective, and gives a similar variation of the potential gradient with increasing impact energy.

Application of an oblique current in conjunction with oblique potential gradient measurement is effective, whether the current is close to the 0° direction or the 90° direction, as shown by the potential gradient increasing with increasing impact energy in the regime of minor damage and decreasing with increasing impact energy in the regime of major damage. This trend is in contrast to that obtained by using current that is not oblique, but is in the plane of the laminate, as described above.

The use of electrical contacts at the edge surfaces is less practical than the use of contacts at the in-plane surface. Thus, unless through-hole contacts are used, the oblique method (figure 2(b)) is recommended, as it is effective whichever is the current direction relative to the surface fiber direction. The through-hole method (figure 2(d)) is similarly effective, but the need to drill holes through the specimen is not very desirable.

The use of silver paint electrical contacts with a reinforcing overlayer of non-conductive epoxy is effective for all the electrical configurations, except that silver epoxy is needed for the through-hole electrical contacts.

The potential method of damage sensing is reliable when (i) the resistance between the current line and the potential gradient line (in the direction perpendicular to these lines) is sufficiently low, as attained when these lines are sufficiently close (up to 45 mm or more in the 0° direction, <15 mm in the 90° direction and <2.1 mm in the through-thickness direction) and (ii) the resistance between the current line and the damage location is sufficiently low, as attained when the distance of separation is sufficiently small (up to 55 mm or more in the 0° direction, and <7.5 mm in the 90° direction). The severe distance limitations in the 90° direction and the requirement of current and voltage contacts at the edge when the current is at the surface and in the 0° direction mean that practical use of the two-dimensional potential method should avoid use of surface current in the 0° direction. However, the oblique configuration is viable for current in any direction.

Acknowledgments

This work was supported in part by Global Contour Ltd through a National Science Foundation SBIR project in which Dr Jaycee H Chung of Global Contour Ltd was the Principal Investigator.

References

- [1] Wolterman R L, Kennedy J M and Farley G L 1993 Fatigue damage in thick, cross-ply laminates with a center hole *Compos. Mater.: Fatigue Fracture* **4** 473–90 (ASTM Special Technical Publication, STP 1156)
- [2] NTSB Advisory 2002 *Eighth Update on NTSB Investigation into Crash of American Airlines Flight 587* (Washington, DC: National Transportation Safety Board) <http://www.ntsb.gov/pressrel/2002/020604.htm>
- [3] De Freitas M, Silva A and Reis L 2000 Numerical evaluation of failure mechanisms on composite specimens subjected to impact loading *Composites B* **31** 199–207
- [4] Rose J L, Rajana K M and Barshinger J N 1996 Guided waves for composite patch repair of aging aircraft *Rev. Prog. Quantitative Nondestruct. Evaluation* **15B** 1291–8
- [5] Sjogren A, Krasnikovs A and Varna J 2001 Experimental determination of elastic properties of impact damage in carbon fibre/epoxy laminates *Composites A* **32** 1237–42
- [6] Abry J C, Bochart S, Chateauminois A, Salvia M and Giraud G 1999 *In situ* detection of damage in CFRP laminates by electrical resistance measurements *Compos. Sci. Technol.* **59** 925–35
- [7] Abry J C, Choi Y K, Chateauminois A, Dalloz B, Giraud G and Salvia M 2001 *In situ* monitoring of damage in CFRP laminates by means of AC and DC measurements *Compos. Sci. Technol.* **61** 855–64
- [8] Ceysson O, Salvia M and Vincent L 1996 Damage mechanisms characterisation of carbon fibre/epoxy composite laminates by both electrical resistance measurements and acoustic emission analysis *Scr. Mater.* **34** 1273–80
- [9] Chu Y-W and Yum Y-J 2001 Detection of delamination in graphite/epoxy composite by electric potential method *Proc.—KORUS 2001, The 5th Korea-Russia Int. Symp. on Science and Technology, Section 5—Mechanics and Automotive Engineering* pp 240–2
- [10] Chung D D L and Wang S 2003 Self-sensing of damage and strain in carbon fiber polymer–matrix structural composites by electrical resistance measurement *Polym. Polym. Compos.* **11** 515–25
- [11] Irving P E and Thiagarajan C 1998 Fatigue damage characterization in carbon fibre composite materials using an electrical potential technique *Smart Mater. Struct.* **7** 456–66
- [12] Kaddour A S, Al-Salehi A R, Al-Hassani S T S and Hinton M J 1994 Electrical resistance measurement technique for detecting failure in CFRP materials at high strain rates *Compos. Sci. Technol.* **51** 377–85
- [13] Kupke M, Schulte K and Schüler R 2001 Non-destructive testing of FRP by DC and AC electrical methods *Compos. Sci. Technol.* **61** 837–47
- [14] Mei Z, Guerrero V H, Kowalik D P and Chung D D L 2002 Mechanical damage and strain in carbon fiber thermoplastic-matrix composite, sensed by electrical resistivity measurement *Polym. Compos.* **23** 425–32
- [15] Muto N, Yanagida H, Nakatsuji T, Sugita M, Ohtsuka Y and Arai Y 1992 Design of intelligent materials with self-diagnosing function for preventing fatal fracture *Smart Mater. Struct.* **1** 324–9
- [16] Muto N, Yanagida H, Nakatsuji T, Sugita M, Ohtsuka Y, Arai Y and Saito C 1995 Materials design of CFGFRP-reinforced concretes with diagnosing function for preventing fatal fracture *Adv. Compos. Mater.* **4** 297–308
- [17] Prabhakaran R 1990 Damage assessment through electrical resistance measurement in graphite fiber-reinforced composites *Exp. Techn.* **14** 16–20
- [18] Schulte K 1993 Damage monitoring in polymer matrix structures *J. Phys. Coll. III* **3** C7 1629–36
- [19] Todoroki A, Kobayashi H and Matuura K 1995 Application of electric potential method to smart composite structures for detecting delamination *JSME Int. J. A* **38** 524–30
- [20] Sugita M, Yanagida H and Muto N 1995 Materials design for self-diagnosis of fracture in CFGFRP composite reinforcement *Smart Mater. Struct.* **4** A52–7
- [21] Wang S, Shui X, Fu X and Chung D D L 1998 Early fatigue damage in carbon fiber composites, observed by electrical resistance measurement *J. Mater. Sci.* **33** 3875–84
- [22] Wang S and Chung D D L 2002 Mechanical damage in carbon fiber polymer–matrix composite, studied by electrical resistance measurement *Compos. Interface* **9** 51–60
- [23] Wang S, Kowalik D P and Chung D D L 2004 Self-sensing attained in carbon fiber polymer–matrix structural composites by using the interlaminar interface as a sensor *Smart Mater. Struct.* **13** 570–92
- [24] Wang S, Mei Z and Chung D D L 2001 Interlaminar damage in carbon fiber polymer–matrix composites, studied by electrical resistance measurement *Int. J. Adh. Adh.* **21** 465–71
- [25] Wang X, Fu X and Chung D D L 1998 Electromechanical study of carbon fiber composites *J. Mater. Res.* **13** 3081–92

- [26] Wang X, Wang S and Chung D D L 1999 Sensing damage in carbon fiber and its polymer–matrix and carbon–matrix composites by electrical resistance measurement *J. Mater. Sci.* **34** 2703–14
- [27] Wang X and Chung D D L 1999 Fiber breakage in polymer–matrix composite during static and dynamic loading, studied by electrical resistance measurement *J. Mater. Res.* **14** 4224–9
- [28] Yoshitake K, Shiba K, Suzuki M, Sugita M and Okuhara Y 2004 Damage evaluation for concrete structures using fiber reinforced composites as self-diagnosis materials *Smart Structures and Materials 2004: Smart Sensor Technology and Measurement Systems (Proc. SPIE vol 5384)* ed E Udd and D Inaudi (Bellingham, WA: SPIE) pp 89–97
- [29] Wang S, Chung D D L and Chung J H 2005 Impact damage of carbon fiber polymer–matrix composites, monitored by electrical resistance measurement *Composites A* **36** 1707–15
- [30] Wang S, Chung D D L and Chung J H 2006 Method of sensing impact damage in carbon fiber polymer–matrix composite by electrical resistance measurement *J. Mater. Sci.* **41** 2281–9
- [31] Wang S, Chung D D L and Chung J H 2005 Self-sensing of damage in carbon fiber polymer–matrix composite by measurement of the electrical resistance or potential away from the damaged region *J. Mater. Sci.* **40** 6463–72
- [32] Wang S, Chung D D L and Chung J H 2005 Effects of composite lay-up configuration and thickness on the damage self-sensing behavior of carbon fiber polymer–matrix composite *J. Mater. Sci.* **40** 561–8
- [33] Wang S and Chung D D L 2005 The interlaminar interface of a carbon fiber epoxy–matrix composite as an impact sensor *J. Mater. Sci.* **40** 1863–7
- [34] Todoroki A, Tanaka Y and Shimamura Y 2004 Multi-probe electric potential change method for delamination monitoring of graphite/epoxy composite plates using normalized response surfaces *Compos. Sci. Technol.* **64** 749–58
- [35] Masson L C and Irving P E 2000 Comparison of experimental and simulation studies of location of impact damage in polymer composites using electrical potential techniques *Proc. SPIE, 5th European Conf. on Smart Structures and Materials* vol 4073, ed P F Gobin and C M Friend (Bellingham, WA: SPIE) pp 182–93
- [36] Angelidis N, Khemiri N and Irving P E 2005 Experimental and finite element study of the electrical potential technique for damage detection in CFRP laminates *Smart Mater. Struct.* **14** 147–54
- [37] Wang D, Wang S, Chung D D L and Chung J H 2006 Comparison of the electrical resistance and potential techniques for the self-sensing of damage in carbon fiber polymer–matrix composites *J. Intell. Mater. Syst. Struct.* at press